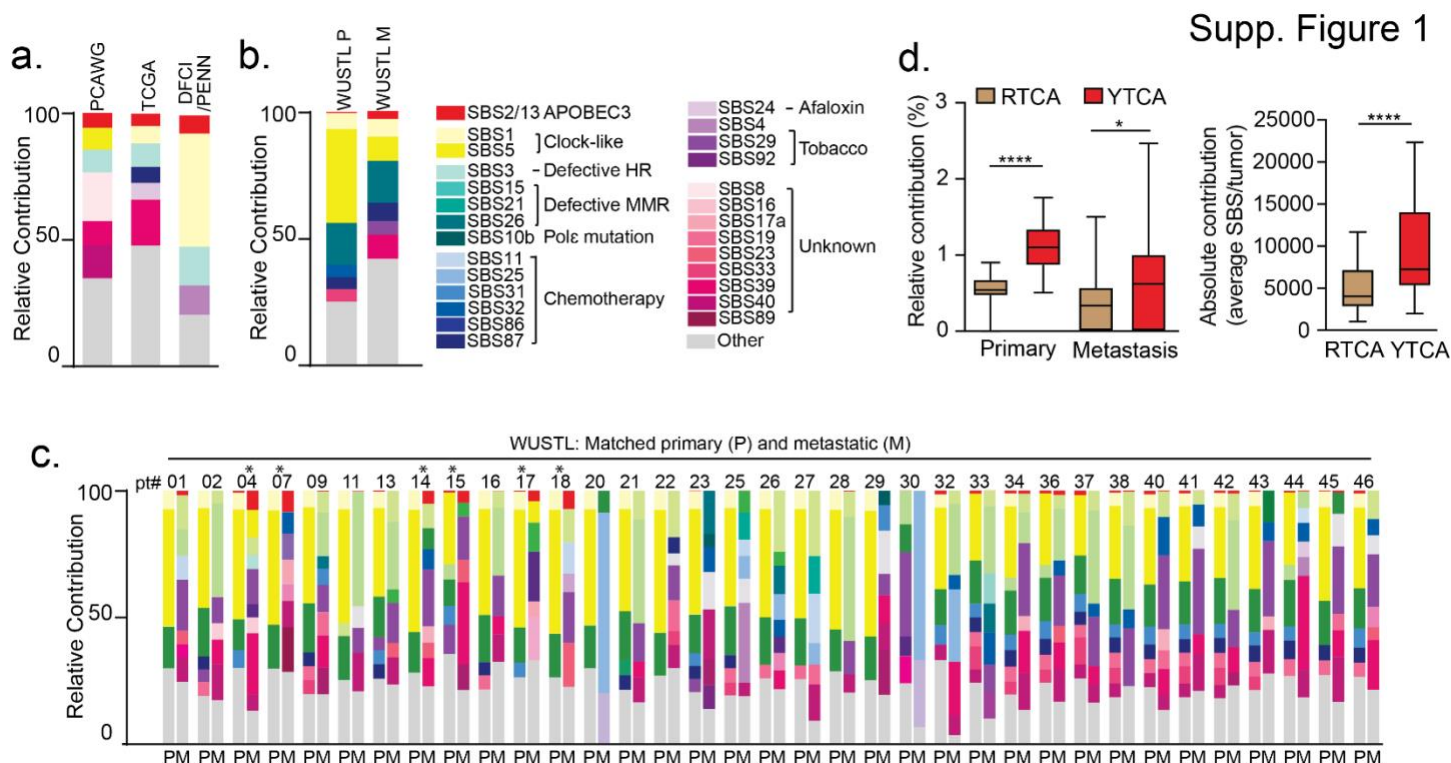
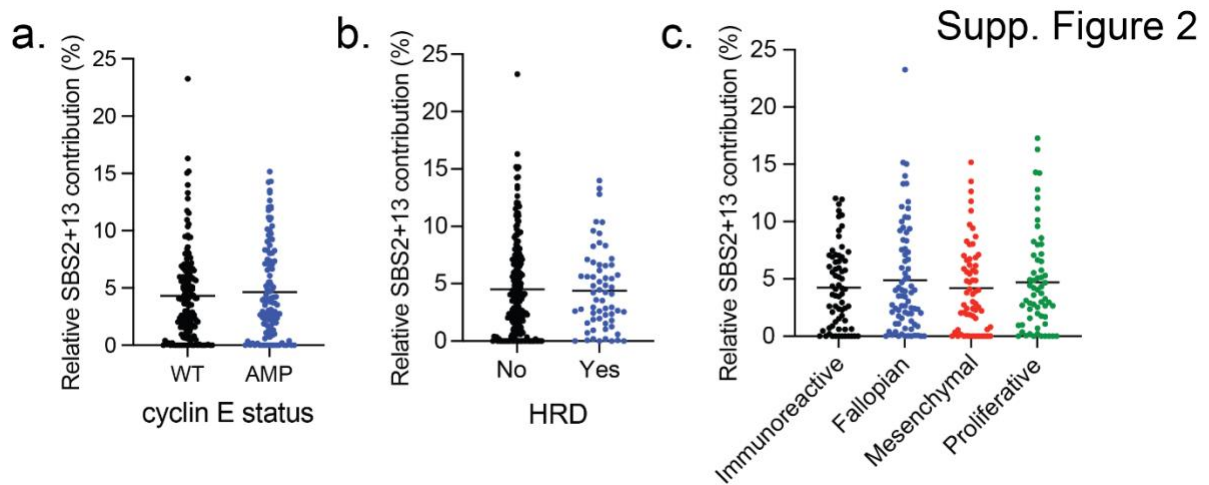


SUPPLEMENTARY FIGURES AND METHODS



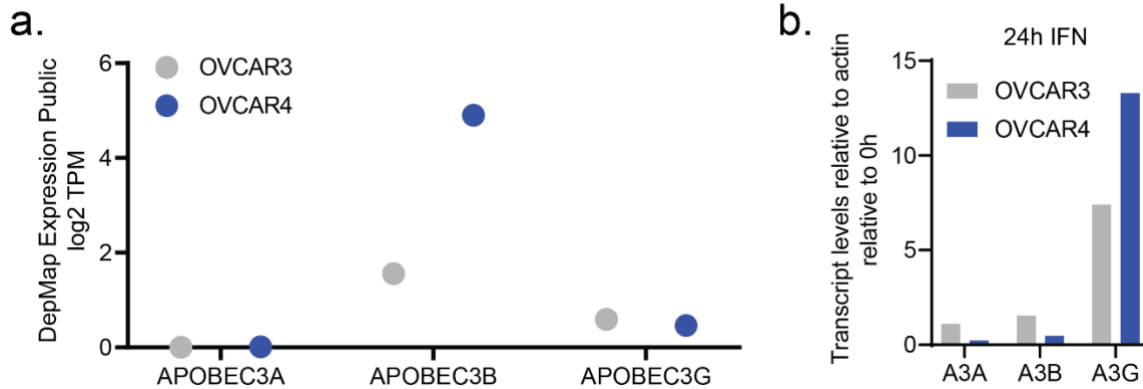
Supp. Figure 1: SBS contribution in HGSC patient genomes. **a)** Whole genome (PCAWG Ovarian Cancer) and whole exome (TCGA Ovarian Cancer, Dana Farber Cancer Institute/University of Pennsylvania) sequencing was assessed to determine the mutational processes occurring within the patient genomes. Relative contribution was determined by assessing the number of mutations identified for each SBS relative to the total mutational burden. Any mutational signature with >5% relative contribution or an increase of >2% in metastatic relative to primary tumors is shown, APOBEC mutational signatures (SBS2 and SBS13) are denoted in red. Gray bars are the combination of all other signatures that were detected at <5% contribution. **b-c)** Whole exome sequencing was assessed to determine the mutational processes occurring with patient genomes from the WUSTL cohort. Any mutational signature with >5% relative contribution is shown, APOBEC mutational signatures (SBS2 and SBS13) are denoted in red. Pooled data for all 35 patients is shown in panel b. Individual primary and metastatic pairs are shown in panel c. Patients with >5% SBS2+13 relative contribution are indicated by * and are highlighted in Figure 1. Legend indicates SBS and proposed etiology for mutational signatures identified to have >5% relative contribution or those that increase by more than 2% in metastatic relative to primary samples. **d)**

Cytosine mutations within SBS2 and SBS13 in WUSTL cohort HGSOC genomes were analyzed for extended sequence context. Quantification shows contribution of mutated cytosines within RTCA or YTCA (R=A or G, Y=T or C) context in primary and metastatic tumors (left), and the absolute contribution of mutations within each context for the entire cohort (right). p-value determined by unpaired t-test; * $p < 0.05$, **** $p < 0.0001$.



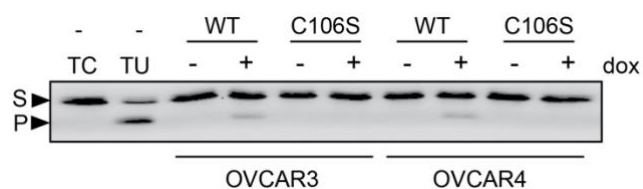
Supp. Figure 2. APOBEC3 mutational signatures do not correlate with genetic or histopathologic HGSOC subtypes. The relative contribution of SBS2 and SBS13 was assessed in HGSOC genomes from TCGA with **a)** amplified or wild type cyclin E, **b)** homologous recombination deficiency (HRD yes) or proficiency (HRD no) as defined by presence of the HRD mutational signature SBS3, **c)** specific molecular subtypes as defined by transcriptional signatures. All statistical comparisons by unpaired one-way Anova were not significant.

Supp. Figure 3



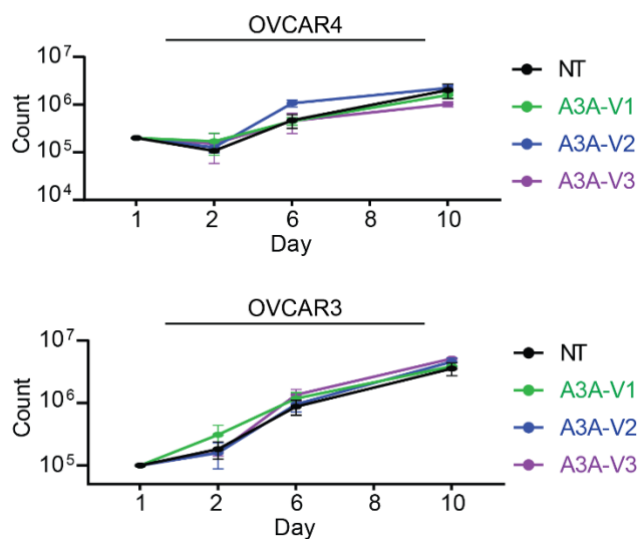
Supp. Figure 3: Endogenous A3A expression is not detected in OVCAR3 and OVCAR4 cells. **a)** DepMAP analysis of *APOBEC3A*, *APOBEC3B*, and *APOBEC3G* gene expression in OVCAR3 and OVCAR4 cell lines (Expression Public 23Q4 database). Values are log₂ transcript count per million (TPM). **b)** OVCAR3 and OVCAR4 cell lines were treated with type I IFN for 24h. Cells were harvested and transcripts for APOBEC3 family members (*A3A*, *A3B*, *A3G*) were assessed relative to untreated controls.

Supp. Figure 4



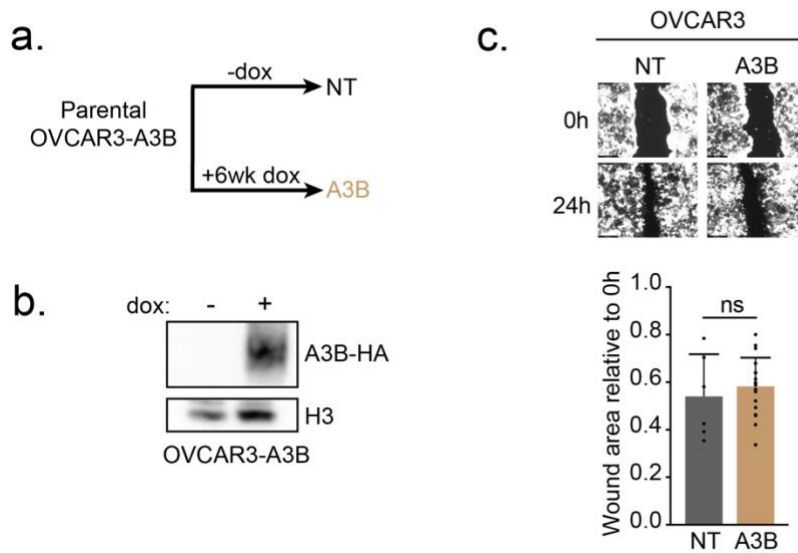
Supp. Figure 4: A3A is active following dox induction. a) Deaminase activity in OVCAR4 and OVCAR3 cells induced with dox to express wild-type (WT) A3A or the catalytic mutant (C106S). Lysates were incubated with a ssDNA oligonucleotide containing a single cytosine. Cytosine deamination followed by addition of uracil-DNA glycosylase (UDG) results in an abasic site; incubation with NaOH results in oligonucleotide cleavage. Substrate (S) and product (P) bands are visualized by gel electrophoresis. Oligonucleotides that contain a single cytosine (TC) or single uracil (TU), incubated in the absence of cell lysate, are used as negative and positive controls, respectively. Image is representative of n=3 biological replicates.

Supp. Figure 5

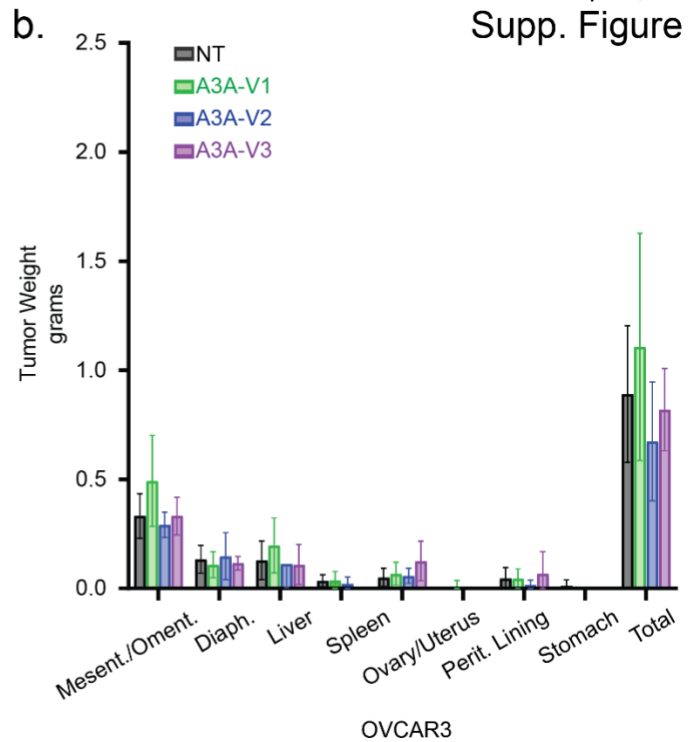
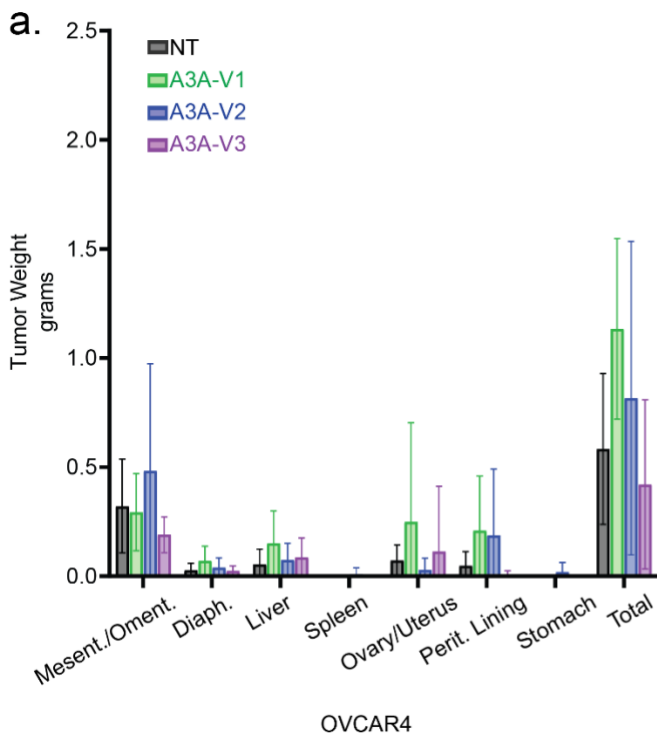


Supp. Figure 5: A3A expression does not alter cellular proliferation in OVCAR4 and OVCAR3 cells. Cells were counted on days 1, 2, 6, 8, and 10 after seeding. NT cells were cultured in parallel and counted at the same time points. Results are mean of biological triplicates. Error bars are standard deviation.

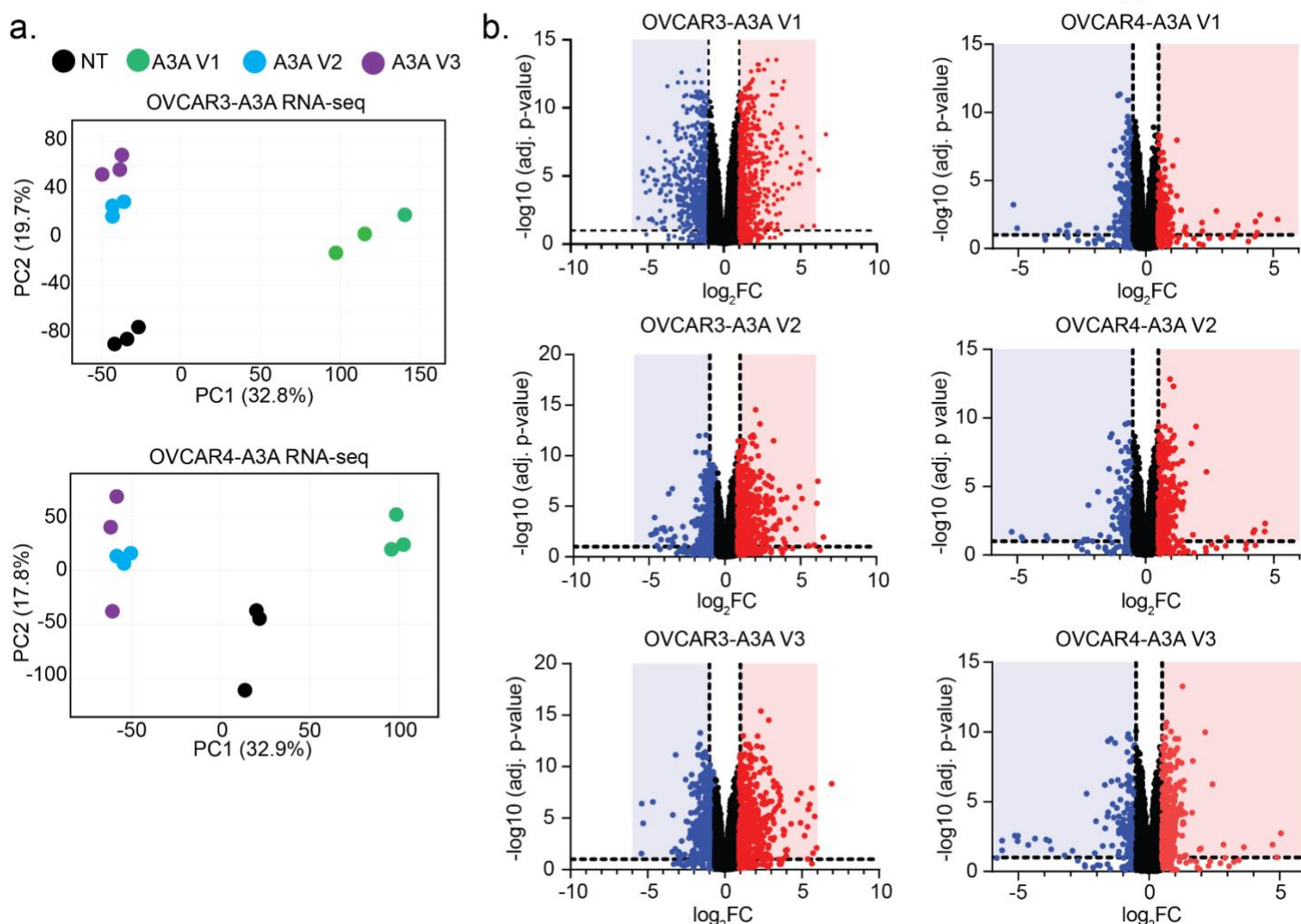
Supp. Figure 6



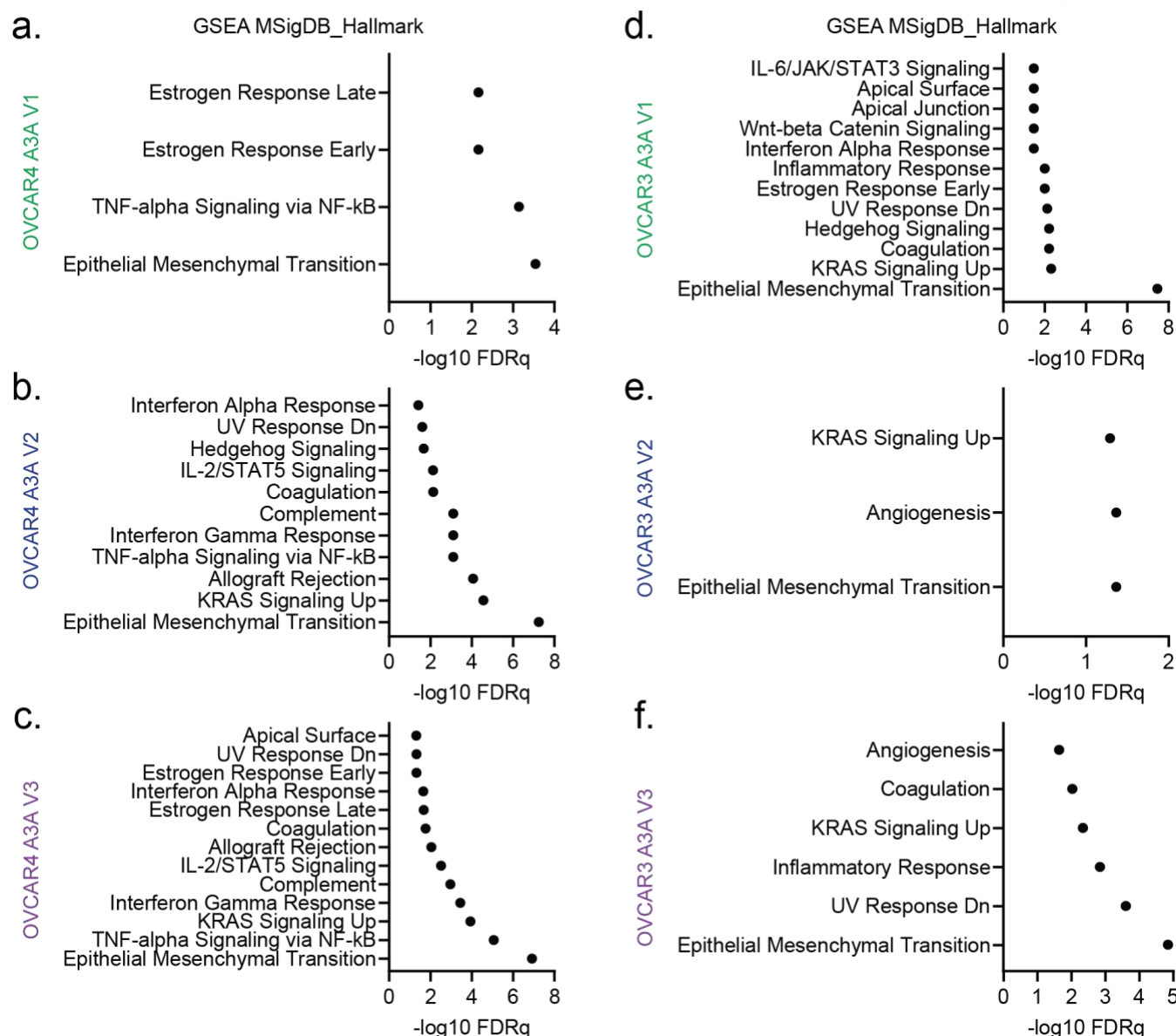
Supp. Figure 6. Intermittent A3B expression does not impact HGSOC cell migration. **a)** OVCAR3-A3B cells were treated with dox per the schema in Figure 2a for 7 weeks. Parental non-treated (NT) cells were cultured in parallel. **b)** Cell lysates collected from OVCAR3-A3B cells after 24 hours of dox treatment were analyzed by immunoblot. Expression of HA-tagged A3B is demonstrated by anti-HA antibody. Histone H3 is loading control. **c)** Wound healing assays were performed to assess the migratory phenotype of OVCAR3-A3B cells. The wound was imaged using a 4x objective at 0h and 24h. Wound area at 24h relative to 0h is shown in bar graph. Significance was determined by unpaired t-test.



Supp. Figure 7. Intraperitoneal tumor burden of OVCAR4 and OVCAR3 tumors. a-b) Tumor nodules were isolated from each organ and weighed. Compiled tumor weight from each organ is shown. Error bars are mean with standard deviation. No statistically significant differences by one-way ANOVA with Dunnett's correction were detected from evaluation of A3A-exposed cells compared to NT.

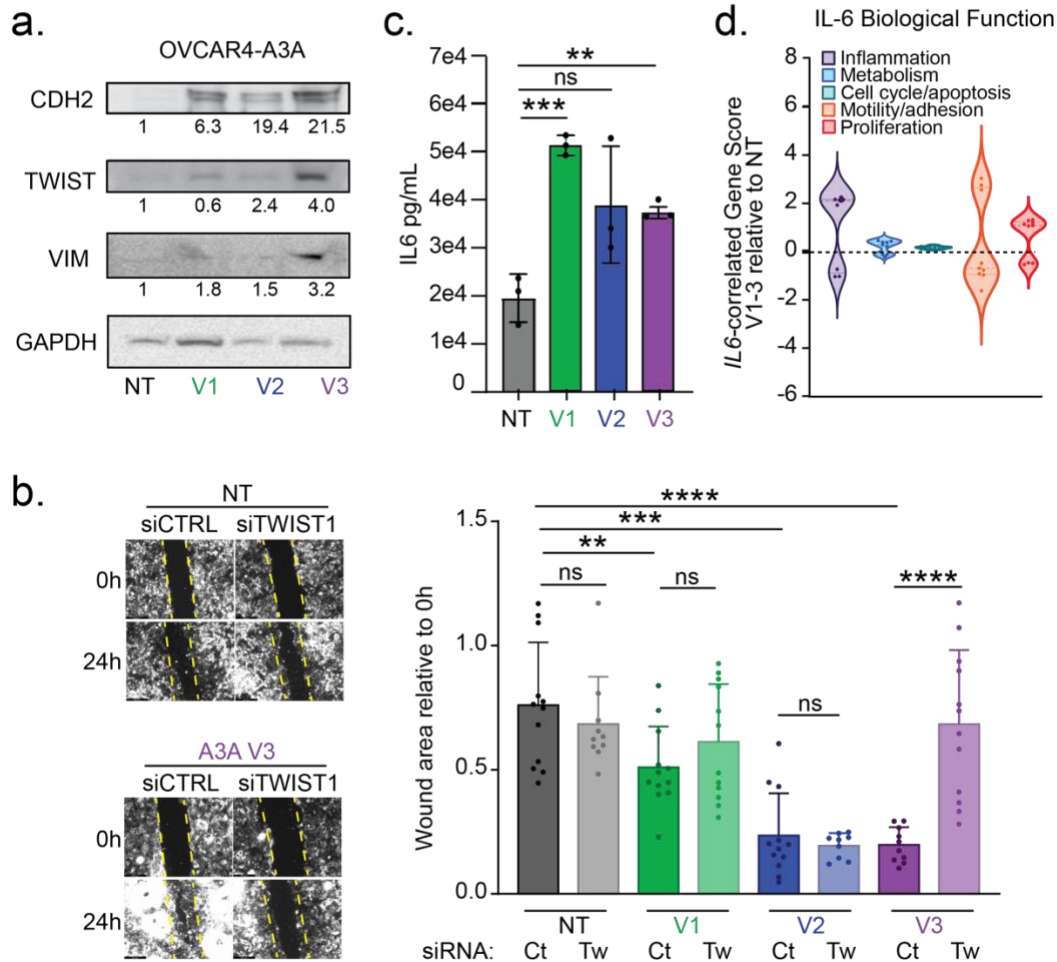


Supp. Figure 8. Gene expression changes elicited by A3A in HGSOC cells. **a)** PCA plot of gene expression in OVCAR3-A3A and OVCAR4-A3A NT and V1-3 show clustering of replicates within each sample and variance among independently-derived cell lines. **b)** Volcano plots based on RNA-sequencing data from OVCAR3-A3A and OVCAR4-A3A cells. Gene expression is plotted for each A3A-exposed version relative to NT cells. Significance threshold is set to adjusted p -value < 0.01 , \log_2 Fold Change (FC) is set to < -1 or > 1 for OVCAR3-A3A and < -0.5 or > 0.5 for OVCAR4-A3A. **c)** Volcano plot based on RNA-sequencing data from WUSTL cohort patients. Differential expression of genes was compared between metastatic sites with APOBEC3 High or APOBEC3 Low mutational burdens as defined in Fig. 1c. Significance threshold is set to adjusted p -value < 0.01 , \log_2 Fold Change (FC) is set to < -1.25 or > 1.25 .



Supp. Figure 9. Gene set alterations elicited by A3A in HGSOc cells. a-f) RNA-seq from OVCAR4 and OVCAR3-A3A V1-3 and NT parental cell lines was performed. Gene set enrichment analysis (GSEA) of the significant differentially expressed genes (DEGs) between A3A-exposed and NT cells was assessed and all significant gene sets identified within the MSigDB Hallmark database are shown. Significance determined by FDR q-value.

Supp. Figure 10



Supp. Figure 10. TWIST depletion mitigates A3A-induced migratory phenotype in OVCAR4 cells. **a)** Immunoblot of mesenchymal markers CDH2, TWIST1, and Vimentin in OVCAR4-A3A V1-3 and NT cells. GAPDH is a loading control. Bands are quantified relative to loading control and normalized to NT lane. **b)** Wound healing assay of OVCAR3-A3A NT and V1-3 cells depleted of *TWIST1* (Tw) by siRNA or treated with non-targeting siRNA control (Ct). Images were acquired with 4x objective, representative images from V3 are shown. Wound area was calculated and is plotted as 24h area relative to 0h. **c)** ELISA for IL-6 detection in the media of OVCAR4-A3A V1-3 and NT cell lines after 3 days in culture. Error bars are mean with SD for n=3 biological replicates. **d)** IL6-correlated gene score defined by gene expression from RNA sequencing of OVCAR4-A3A V1-3 cell lines. For all panels, significance was determined by ordinary one-way ANOVA with Dunnett's correction for multiple comparisons for group analysis. For comparisons between two groups significance was determined by unpaired t test; **p<0.01, ***p<0.001, ****p<0.0001.

SUPPLEMENTARY METHODS & REFERENCES

DepMap APOBEC3 expression analysis. Published expression data for OVCAR4 and OVCAR3 cell lines was first assessed using DepMap Portal for *APOBEC3A*, *APOBEC3B*, and *APOBEC3G* gene expression in the Expression Public23Q4 database.

CyclinE amplification and Defective Homologous Recombination. CyclinE (*CCNE*) amplification was defined using the annotated structural variants. A sample was classified as CyclinE amplified when the copy number values at *CCNE* genomic regions were more than 2. Similarly, wild-type cyclinE was defined as tumors whose *CCNE* copy number values were equal to 2. On the other hand, tumors with SBS3 attribution more than 0 (resulted from the signature extraction discussed in Methods) would be classified as having defective homologous recombination.

Deaminase assay. OVCAR4-A3A and OVCAR3-A3A cells were treated with doxycycline for 24 hours then collected by centrifugation and lysed in a buffer containing 1X RIPA buffer (Cell Signaling Technology) with the addition of 1X Pierce protease inhibitor (EDTA Free, Thermo Scientific) and PMSF (GoldBio) on ice for ten minutes followed by brief sonication. Protein concentration was determined by Bradford assay. A deaminase reaction buffer containing 20mM MES and 0.1% Tween was prepared in water and the pH was adjusted to 5.9-6.1. Cell lysate was combined with reaction buffer and an oligo containing a single cytosine base (TGAGGAATGAAGTTGATTCAAATGTGATGAGGTGA) with a 5'-FAM fluorophore as previously described(1). The negative control reaction consisted of the buffer and single-cytosine oligo, the positive control contained an identical oligo with a uracil in place of the cytosine. All samples and control reactions were incubated at 37°C for 2h, followed by the addition of 2.5 units of uracil DNA glycosylase (NEB) and subsequent at 37°C for 15m. A loading dye solution containing formamide, sodium hydroxide, and EDTA with bromophenol blue was added and reactions were boiled at 95°C for 15m. Reactions were run out on a urea-acrylamide gel in 1X TBE and the gel was imaged using the fluorescein channel on a Bio-Rad ChemiDoc MP imager.

REFERENCES

1. DeWeerd R, and Green AM. Qualitative and Quantitative Analysis of DNA Cytidine Deaminase Activity. *Methods Mol Biol.* 2022;2444:161-9.